

Article

Thermodynamic Analysis of CNG Fast Filling Process of Composite Cylinder Type IV

Adam Saferna ¹, Piotr Saferna ¹, Szymon Kuczyński ^{1,2,*} , Mariusz Łaciak ² , Adam Szurlej ² and Tomasz Włodek ^{1,2} 

¹ Techplast Sp. z o.o., Krakowska 83 P, 34-120 Andrychów, Poland; adam.saferna@techplast.net (A.S.); piotr.saferna@techplast.net (P.S.); twlodek@agh.edu.pl (T.W.)

² Gas Engineering Department, Drilling, Oil and Gas Faculty, AGH University of Science and Technology, Mickiewicza 30 Av., 30-059 Kraków, Poland; laciak@agh.edu.pl (M.Ł.); szua@agh.edu.pl (A.S.)

* Correspondence: szymon.kuczynski@agh.edu.pl

Abstract: Due to ecological and economic advantages, natural gas is used as an alternative fuel in the transportation sector in the form of compressed natural gas (CNG) and liquefied natural gas (LNG). Development of infrastructure is necessary to popularize vehicles that use alternative fuels. Selected positive factors from EU countries supporting the development of the CNG market were discussed. The process of natural gas vehicle (NGV) fast filling is related to thermodynamic phenomena occurring in a tank. In this study, the first law of thermodynamics and continuity equations were applied to develop a theoretical model to investigate the effects of natural gas composition on the filling process and the final in-cylinder conditions of NGV on-board composite cylinder (type IV). Peng–Robinson equation of state (P-R EOS) was applied, and a lightweight composite tank (type IV) was considered as an adiabatic system. The authors have devised a model to determine the influence of natural gas composition on the selected thermodynamic parameters during fast filling: Joule–Thomson (J-T) coefficient, in-cylinder gas temperature, mass flow rate profiles, in-cylinder mass increase, natural gas density change, ambient temperature on the final natural gas temperature, influence of an ambient temperature on the amount of refueled natural gas mass. Results emphasize the importance of natural gas composition as an important parameter for the filling process of the NGV on-board composite tank (type IV).

Keywords: compressed natural gas; alternative fuels; CNG tank; composite cylinder fast filling; composite tank (type IV), energy storage



Citation: Saferna, A.; Saferna, P.; Kuczyński, S.; Łaciak, M.; Szurlej, A.; Włodek, T. Thermodynamic Analysis of CNG Fast Filling Process of Composite Cylinder Type IV. *Energies* **2021**, *14*, 5568. <https://doi.org/10.3390/en14175568>

Academic Editor: Muhammad Abdul Qyum

Received: 21 June 2021

Accepted: 30 August 2021

Published: 6 September 2021

Publisher's Note: MDPI stays neutral with regard to jurisdictional claims in published maps and institutional affiliations.



Copyright: © 2021 by the authors. Licensee MDPI, Basel, Switzerland. This article is an open access article distributed under the terms and conditions of the Creative Commons Attribution (CC BY) license (<https://creativecommons.org/licenses/by/4.0/>).

1. Introduction

Natural gas is widely used in industry, energy sector, and residential. Due to ecological and economic advantages, natural gas is also increasingly used as an alternative fuel in the transportation sector in the form of compressed natural gas (CNG) and liquefied natural gas (LNG). The history of gaseous fuels used in internal combustion engines begins in 1860s when the French inventor Etienne Lenoir constructed the first two-stroke engine powered by a mixture of town gas and air [1]. Since then, gaseous fuels have been used to power vehicles, and they were the most popular in times of crisis related to the shortage of conventional fuels [2,3]. A dynamic increase in the number of natural gas vehicles (NGV) has been observed. In 2020, there were over 28.5 million vehicles. The world leader in the use of CNG in transport is China, with over 6.7 million NGV vehicles, the next place Iran 4.9 million, and India with 3.3 million NGVs. The EU leaders are Italy with 1.1 million NGV, Germany with 98,200 NGV, and Bulgaria with 69,800 NGV [4].

Changes in the global natural gas market have been observed in recent years, including a significant increase in unconventional natural gas production, as well as the importance of LNG technology in international natural gas trading, which caused a decrease in natural gas prices [5–7]. In Poland, significant projects are planned, ongoing, or have been completed

to diversify natural gas supplies, including the LNG terminal in Świnoujście [8–10]. Thus, it can be assumed that the use of natural gas as an alternative fuel in transport will be one of the prospective segments of the Polish natural gas market.

To mitigate the environmental impact of transport, infrastructure development is necessary to popularize vehicles that use electricity and other alternative fuels. Directive 2014/94/EU of the European Parliament and of the Council on alternative fuels infrastructure obliges Member States to deploy electricity charging infrastructure, refueling stations for hydrogen and refueling stations for natural gas, including biomethane (RNG), in gaseous form (CNG) and liquefied form (LNG) [11]. In terms of other alternative fuels (biofuels, synthetic fuels), it remains up to the Member States. Natural gas infrastructure should be deployed along the Trans-European Transport Network (TEN-T) by 2025 and in urban and suburban areas [12]. The European Green Deal, published in December 2019, presents the need to accelerate the shift towards sustainable and smart transport and the use of alternative transport fuels [13]. NGVs require durable, lightweight, and safe tanks to maintain regular vehicle size, weight, and driving range.

Natural gas as a transportation fuel has the potential to reduce emissions, and it is justified to use compressed natural gas for transport purposes [14,15]. Development of tank design can contribute to vehicle weight reduction and thus fuel consumption reduction. High pressure cylinder design for the on-board storage of natural gas as fuel for vehicles includes: (i) type I, which are made of metallic materials; (ii) type II, which has a metal liner and hoop-wrapped composite reinforcement; (iii) type III, which has a metal liner and a full wrapped composite reinforcement, and (iv) type IV, which have a non-metallic, non-load sharing liner and a composite reinforcement on both the cylindrical part and dome ends [16]. The advantage of using materials such polymers and fiber composites for alternative fuel tanks is that they are light while offering high shock resistance and long life.

The process of vehicle tank fast refueling lasts approx. 5 min. The standard service pressure of the tank in the vehicle is 200 bar (the maximum pressure should not exceed 260 bar). The tanks are designed and tested to be refueled 1000 times a year during its operation in the temperature range from $-40\text{ }^{\circ}\text{C}$ to $65\text{ }^{\circ}\text{C}$ with the possibility of temporary temperature increase to $82\text{ }^{\circ}\text{C}$ [16–18].

A few researchers have addressed the problem of modelling and thermodynamic analysis of the filling process of cylinders with compressed natural gas. Kuntz modeled the fast filling process of the tank with compressed natural gas based on the first law of thermodynamics [19]. Farzaneh-Gord et al. studied the temperature effects on natural gas in NGV cylinder during the fast filling process. The ideal and real gas were compared using the Peng–Robinson equation of state (PR EOS), for the one-component system-methane, which is the main component of natural gas [20,21]. Deymi-Dashtebayaz et al. modeled a dynamic fast filling process of compressed natural gas to the vehicle's cylinder using PR EOS for methane. They investigated the influence of the initial pressure of the storage reservoir on methane parameters in NGV cylinder at target pressure [22]. In another manuscript, Farzaneh-Gord et al. presents the analysis of the reservoirs pressures and temperatures on the performance of the cascade fueling station and compares these effects between one-component systems: methane and hydrogen [23,24]. In 2014, Nahavandi and Farzaneh-Gord investigated the flow and heat transfer during filling in natural gas vehicle's onboard cylinder type III. They employed Redlich–Kwong equation of state to determine the thermodynamic properties of methane [25]. Deymi-Dashtebayaz et al. determined heat transfer rate between in-cylinder flow and inner surface of cylinder wall and developed a thermodynamic method to predict gas pressure and temperature variations inside the cylinder and cylinder wall temperature during the refueling. On-board storage cylinders types I and III were considered [26]. In their carefully designed study, Farzaneh-Gord et al. provided a detailed theoretical analysis of the natural gas composition effects on the filling process of an onboard natural gas vehicle cylinder for methane and selected Iran natural gas compositions. Calculations were performed with AGA8 EOS [27]. Khamfroush

et al. developed the model of compression process of real natural gas and compared with real data from CNG filling station. The polytropic work of a three-stage compressor was considered [28]. Ramoutar offers a comprehensive thermodynamic analysis of Natural Gas Vehicle cylinder refueling from a cascade reservoir using chilled natural gas and studied the temperature effects on cylinder fill ratio [29]. There is a limited number of researchers and research groups in the field of cylinder filling process modelling. Other research groups, i.e., Zhang et al., studied the fast refill of compressed natural gas with active heat removal and Taccani et al. performed analysis of the loading and unloading system of a CNG carrier, equipped with lightweight cylinders [30,31].

Despite the interest in the modelling of cylinder filling with compressed natural gas, there are also studies which have considered thermodynamic parameters during hydrogen fast filling to cylinders (types III and IV) [32–42].

In this study, the main objective is to investigate the effects of natural gas composition on an NGV on-board cylinder during the fast filling process. It was assumed that, during filling, a lightweight cylinder (type IV) is connected to one reservoir tank. The theoretical model was developed based on the mass and energy balance. Thermodynamic properties of natural gas in the cylinder were calculated for selected time steps during the filling process. The thermodynamic properties of natural gas mixtures are computed based on P-R EOS and thermodynamics relationships. The influence of selected natural gas compositions that occur in Polish gas transmission and distribution systems, has been analyzed for its impact on the fast filling process.

2. Natural Gas Composition

Natural gas is a mixture of components with different properties, and therefore, the thermodynamic properties of natural gas depend on their individual components. To know the detailed natural gas properties during cylinder filling, the influence of its composition should be considered. For this purpose, the Peng–Robinson equation of state (PR EOS) was applied.

Presented in Table 1, the gas samples are similar in composition to the real natural gas which occurs in the Polish natural gas transmission system. Natural gas in Poland has different compositions which results from the genesis of natural gas. The natural gas produced in the southern part of Poland (high-methane gas) has a different composition in comparison to the gas supplied by the LNG terminal located in Świnoujście—northwest of Poland (natural gas with a high content of ethane). In addition, nitrogen-rich natural gas composition (Gas sample 5) which occurs in western Poland, is different due to production from nitrogen-rich natural gas reservoirs located in the western part of Poland. Therefore, CNG refueling stations, feed from various outlet points of the transmission/distribution system, located in different places in Poland may differ slightly in composition (except for nitrogen-rich gas). In addition, a hypothetical composition with the use of 3% hydrogen in a mixture with methane was also considered (Gas sample 6) due to the development of hydrogen technology and the recognition of hydrogen as one of the main energy carriers in the future. To compare the calculation results with other studies, pure methane (Gas sample 1) was also investigated. Gas sample 4 is an example of natural gas with heavier additives (propane and butanes).

Selected for this research, real natural gas mixtures (Gas samples 2, 3, 5) may be available at the refueling stations, which can be filled at the fast-refueling stations to composite tanks (type IV) installed in NGV.t

Table 1. Mole fraction of natural gas from various outlet points of the transmission system in Poland (Gas samples 2,3,5) and other gas samples.

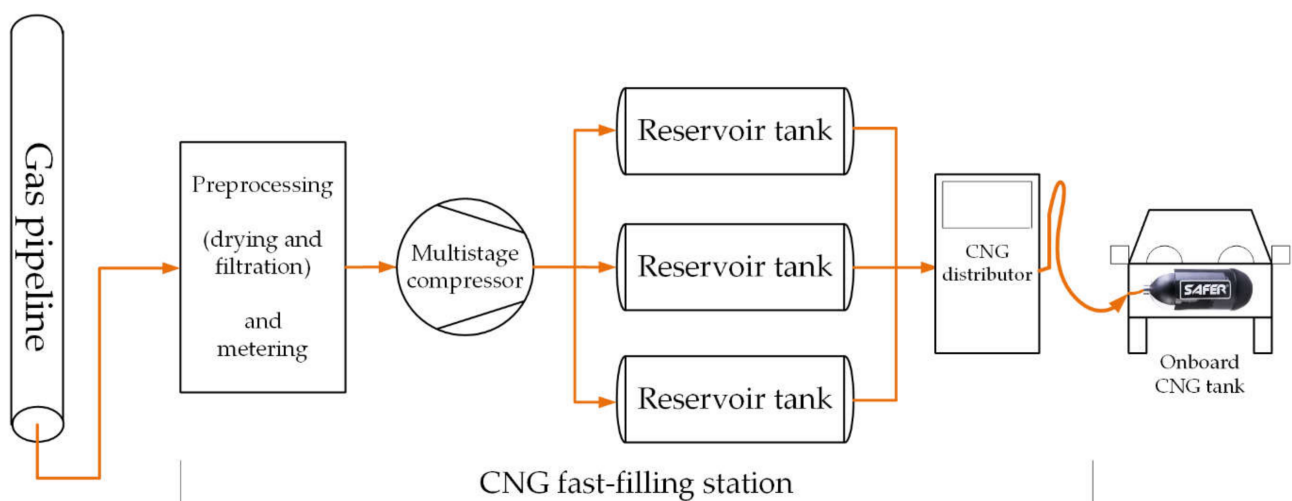
Component	Chemical Formula	Gas Sample No.					
		1	2	3	4	5	6
		Concentration, [% Mol]					
methane	CH ₄	100	96.2	93.3	90	80.3	97
ethane	C ₂ H ₆	-	2.6	6.3	6.5	0.3	-
propane	C ₃ H ₈	-	1.1	0.3	2.5	-	-
butane	n-C ₄ H ₁₀	-	-	-	0.5	-	-
isobutane	i-C ₄ H ₁₀	-	-	-	0.5	-	-
nitrogen	N ₂	-	0.1	0.1	-	19.4	-
hydrogen	H ₂	-	-	-	-	-	3

3. CNG Filling Station

There are two types of CNG infrastructure: time-fill and fast-fill. The main differences between those two systems are: (i) available storage capacity and (ii) size of the compressor. These factors determine the amount of fuel dispensed and the time it takes for CNG to be fueled. The problem of long-time filling was solved by the infrastructure that allows filling the NGV tank in time like vehicle refueling with gasoline or diesel (filling time less than 300 s). The filling time of an NGV tank in less than 300 s can be described as fast fill.

Fast filling process of a composite cylinder (type IV) with compressed natural gas.

To increase the utilization of compressor and reservoir tanks, CNG fast filling stations operates in a buffer or cascade storage system and the reservoir tanks are arranged to increase the pressure [43,44]. Figure 1 shows a schematic diagram of a cascade CNG fast filling system. During the fast-filling process of a composite tank (type IV) installed in an NGV, it is connected to a low-pressure reservoir tank. When the gas flow rate reaches a predetermined rate, the system switches to the medium pressure tank and finally to the high-pressure tank to complete filling. As a result, the high-pressure storage tank always operates at a maximum pressure, ensuring that NGVs are always filled with the maximum available gas flow rate. For calculation purposes, it was assumed that the pressure in the reservoir tank is not changing during the fast-filling process of the composite tank (type IV).

**Figure 1.** Scheme of the fast-filling process (cascade storage) of the composite tank (type IV).

4. Thermodynamic Analysis of a CNG Composite Tank (Type IV) Fast Filling Process

To perform calculations and to develop a thermodynamic model of the composite tank (type IV) fast filling process, it was assumed that a composite CNG tank (type IV), installed in an NGV, is considered as an open thermodynamic system that goes through a quasi-static filling process. To determine the selected thermodynamic parameters, the continuity equation and the first law of thermodynamics were applied. Another assumption was to assume a constant volume of the composite tank (type IV) which has only one entry point (inlet). Based on the above assumptions, the continuity equation (conservation of mass principle) can be written in the form of Equation (1):

$$\dot{m}_i = \frac{dm_c}{dt} \quad (1)$$

In Equation (1), \dot{m}_i is the inlet mass flow rate which can be calculated as natural gas expansion in the orifice (cylinder inlet) [19,27].

$$\dot{m}_i = C_d \cdot \rho_R \cdot A_{orifice} \cdot \left(\frac{P_C}{P_R}\right)^{1/\gamma} \cdot \left\{ \left(\frac{2\gamma}{\gamma-1}\right) \left(\frac{P_R}{\rho_R}\right) \left[1 - \left(\frac{P_C}{P_R}\right)^{\gamma-1/\gamma}\right] \right\}^{1/2} \quad (2)$$

if:

$$\frac{P_C}{P_R} \leq \left(\frac{2}{\gamma+1}\right)^{\gamma/\gamma-1}$$

$$\dot{m}_i = C_d \sqrt{\gamma P_R \rho_R} A_{orifice} \left(\frac{2\gamma}{\gamma-1}\right)^{\gamma+1/2(\gamma-1)} \quad (3)$$

if:

$$\frac{P_C}{P_R} > \left(\frac{2}{\gamma+1}\right)^{\frac{\gamma}{\gamma-1}}$$

Equation (2) is valid for subsonic flow, while Equation (3) is for sonic conditions. The discharge coefficient C_d was introduced to account the irreversibility of the flow through the orifice. The first law of thermodynamics for a specific volume of a composite tank can be written in general form as the following Equation (4):

$$\dot{Q}_{cv} + \sum \dot{m}_i \left(h_i + \frac{V_i^2}{2} + gz_i \right) = \sum \dot{m}_e \left(h_e + \frac{V_e^2}{2} + gz_e \right) + \frac{d}{dt} \left[m \left(u + \frac{V^2}{2} + gz \right) \right]_{cv} + \dot{W}_{cv} \quad (4)$$

The work in the filling process is equal to zero and therefore the potential energy and kinetic energy change in the NGV composite tank $\left(\frac{V^2}{2}\right)_{cv}$ can be neglected. The equation can be simplified as shown below:

$$\frac{dU_C}{dt} = \dot{Q} + \dot{m}_i \left(h_i + \frac{V_i^2}{2} \right) \quad (5)$$

By applying the energy balance equation for the reservoir tank, it was obtained $h_i + \frac{V_i^2}{2} = h_R$. In this case, it is assumed that the conditions of the reservoir tank do not change, so h_R remains constant during the filling process. By substituting h_R into Equation (5), the following equation was obtained:

$$\frac{dU_C}{dt} = \dot{Q} + \dot{m}_i h_R \quad (6)$$

The heat loss from the NGV composite tank to the environment can be written as:

$$\dot{Q} = -U_{HC} A_C (T_C - T_{amb}) \quad (7)$$

Heat transfer coefficient of the composite tank U_{HC} represents the heat exchange rate between natural gas in the cylinder and the environment. A higher U_{HC} value means a lower final in-cylinder condition. Combining Equations (1), (6), and (7), the following equation was obtained:

$$\frac{d(m_C u_C)}{dt} = -U_{HC} A_C (T_C - T_{amb}) + \frac{dm_C}{dt} h_R \quad (8)$$

or after transformation:

$$\frac{d(m_C u_C)}{dt} - \frac{d}{dt}(m_C h_R) = -U_{HC} A_C (T_C - T_{amb}) \quad (9)$$

The above equation can be transformed to the following form:

$$d(m_C u_C - m_C h_R) = -U_{HC} A_C (T_C - T_{amb}) dt \quad (10)$$

Equation (10) was integrated within the limits from the start of the integration process “s” to the next time step of the filling process “r”, as shown in Equation (11):

$$\int_s^r d(m_C u_C - m_C h_R) = - \int_0^t U_{HC} A_C (T_C - T_{amb}) dt \quad (11)$$

The result of integration for one reservoir tank of the fast-filling station is shown below:

$$m_{C_r} (u_C - h_R) - m_{C_s} (u_C - h_R) = -U_{HC} A_C \cdot T_{av} t \quad (12)$$

where

m_{C_r} —the mass of natural gas filled for the “last/recent” step;

m_{C_s} —the mass of natural gas filled at the “start” of the filling process;

The average temperature difference between the composite tank and the environment ΔT_{av} is defined as:

$$\Delta T_{av} = \frac{1}{t} \int_0^t (T_C - T_{amb}) dt \quad (13)$$

Finally, the first law of thermodynamics for the filling of a composite tank installed in NGV can be written in the form of Equation (14):

$$u_C = h_R - \frac{U_{HC} A_C \Delta T_{av} t}{m_{C_r}} + \frac{m_{C_s}}{m_{C_r}} (m_{C_s} - h_R) \quad (14)$$

Equations (2), (3), and (14) can be applied to calculate the thermodynamic properties of natural gas (density and internal energy) in a composite tank at any time during the filling process. In the case of an adiabatic system, Equation (14) can be simplified and written as:

$$u_C = h_R + \frac{m_{C_s}}{m_{C_r}} (U_{C_s} - h_R) \quad (15)$$

If $m_{C_s} = 0$, the following relationship is valid at any time during the composite tank filling process:

$$u_C = h_R \quad (16)$$

5. Calculation of Natural Gas Thermodynamic Properties

As mentioned in the previous chapter of this study, it is necessary to determine several thermodynamic parameters of natural gas to analyze the filling process of the composite tank. These parameters are i.e., density (or specific volume) and internal energy. This

chapter explains how these properties were calculated. Detailed methods for calculating most of the thermodynamic parameters of natural gas can be found in [26,27,45,46].

5.1. Peng–Robinson Equation of State

The Peng–Robinson equation of state (PR EOS) is one of the most popular equations for describing the PVT (Pressure-Volume-Temperature) behavior of real pure substances and their mixtures. This equation has the following form as seen in Equation (17) [47]:

$$p = \frac{RT}{v - b_m} - \frac{a_m}{v(v + b_m) + b_m(v - b_m)} \quad (17)$$

Parameters a_m and b_m are defined by classical mixing rules:

$$a_m = \sum_i \sum_j z_i z_j a_{m,i,j} \quad (18)$$

$$b_m = \sum_i z_i b_i \quad (19)$$

Other parameters of the PR EOS are defined as:

$$a_{m,i,j} = (1 - \delta_{ij}) \cdot \sqrt{a_i \alpha_i a_j \alpha_j} \quad (20)$$

$$\alpha_i = \left[1 + \kappa_i \left(1 - \sqrt{\frac{T}{T_{cr,i}}} \right) \right]^2 \quad (21)$$

where

$$\kappa_i = 0,379642 + 148503\omega_i - 0,164423\omega_i^2 + 0,016666\omega_i^3 \quad (22)$$

$$a_i = 0,45724 \cdot \frac{R^2 T_{cr,i}^2}{p_{cr,i}} \quad (23)$$

$$b_i = 0,07780 \cdot \frac{R T_{cr,i}}{p_{cr,i}} \quad (24)$$

In the PR EOS, the compressibility factor Z is defined as:

$$Z^3 + (B - 1)Z^2 + (A - 3B^2 - 2B)Z + (B^3 + B^2 - AB) = 0 \quad (25)$$

where PR EOS dimensionless coefficients are determined according to the following formula:

$$A = \frac{a_m p}{R^2 T^2} \quad (26)$$

$$B = \frac{b_m p}{RT} \quad (27)$$

From the general form of the real gas equation of state, the molar density can be determined:

$$\rho_m = \frac{p}{ZRT} \quad (28)$$

5.2. Enthalpy and Joule–Thomson Coefficient Calculation

Enthalpy (h) was determined according to Equation (29)

$$h = h_{id} + h_{res} \quad (29)$$

where h_{res} is the residual enthalpy given by the following formula:

$$h_{res} = RT(Z - 1) + \frac{T \frac{da_m}{dT} - a_m}{2\sqrt{2}b_m} \cdot \ln \left[\frac{Z + (1 + \sqrt{2})B}{Z + (1 - \sqrt{2})B} \right] \quad (30)$$

and h_{id} is the ideal gas enthalpy calculated from a given polynomial function [47]:

$$h_{id} = A \cdot \frac{T}{1000} + \frac{B \cdot \left(\frac{T}{1000}\right)^2}{2} + \frac{C \cdot \left(\frac{T}{1000}\right)^3}{3} + \frac{D \cdot \left(\frac{T}{1000}\right)^4}{4} - \frac{1000 \cdot E}{T} + F - H + h_{id298.15K} \quad (31)$$

where

A, B, C, D, E, F, H —empirical coefficients;

T —temperature [K]/1000;

$h_{id298.15K}$ —ideal gas enthalpy in 298.15 K;

Calculated change of the compressibility factor Z during the composite tank (type IV) filling process with the considered natural gas mixtures and gas samples is presented on Figure 2.

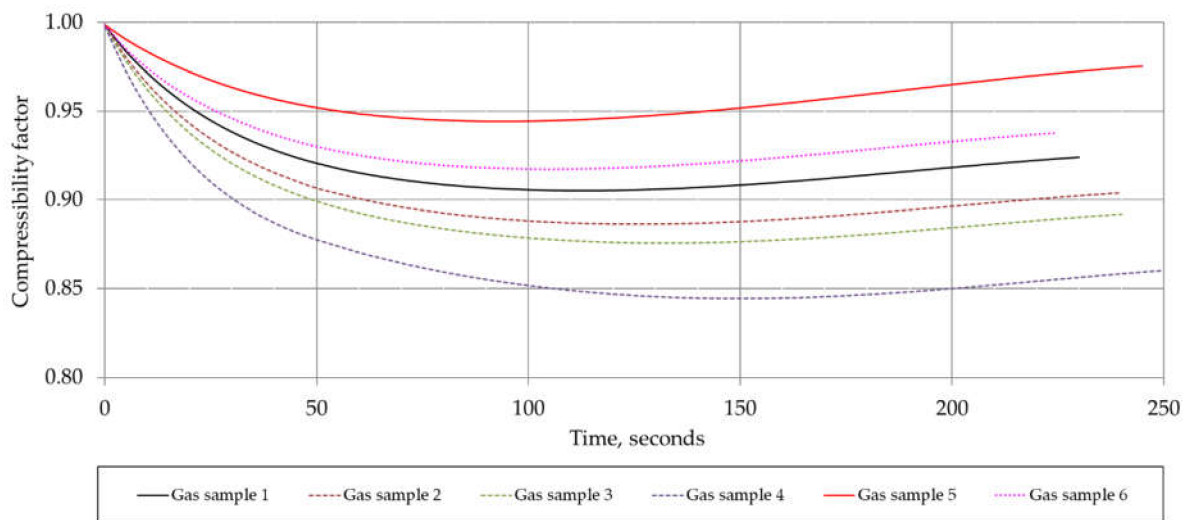


Figure 2. Change of the compressibility factor Z during the filling process of the composite tank (type IV) for the considered natural gas mixtures and samples.

Isobaric heat capacity was determined according to Equation (32):

$$C_p = C_{pid} + C_{pr} \quad (32)$$

where

$$C_{pres} = R \cdot \left(T \left(\frac{\partial Z}{\partial T} \right)_p + Z - 1 \right) + \frac{T \frac{da_m}{dT} - a_m}{2\sqrt{2}b_m} \cdot \left[\frac{\left(\frac{\partial Z}{\partial T} \right)_p + (1 + \sqrt{2}) \left(\frac{\partial B}{\partial T} \right)_p}{Z + (1 + \sqrt{2})B} - \frac{\left(\frac{\partial Z}{\partial T} \right)_p - (\sqrt{2} - 1) \left(\frac{\partial B}{\partial T} \right)_p}{Z - (1 - \sqrt{2})B} \right] + \frac{T \frac{d^2 a_m}{dT^2} - a_m}{2\sqrt{2}b_m} \cdot \ln \left[\frac{Z + (1 + \sqrt{2})B}{Z + (1 - \sqrt{2})B} \right] \quad (33)$$

Ideal gas heat capacity C_{pid} is calculated from empirical polynomial functions [48]:

$$C_{pid} = A + B \cdot \left(\frac{T}{1000} \right) + C \cdot \left(\frac{T}{1000} \right)^2 + D \cdot \left(\frac{T}{1000} \right)^3 + \frac{E}{\left(\frac{T}{1000} \right)^2} \quad (34)$$

Joule–Thomson coefficient is defined with the application of PR EOS according to the following Equation (35):

$$\mu_{J-T} = \left(\frac{\partial T}{\partial P} \right)_h = \frac{1}{C_p} \left[T \left(\frac{\partial v}{\partial T} \right)_p - v \right] = \frac{1}{C_p} \left[T \left(\frac{R}{p} \left(T \left(\frac{\partial Z}{\partial T} \right)_p + Z \right) \right) - v \right] \quad (35)$$

5.3. Internal Energy Calculation

By assuming that the internal energy is a function of temperature and molar specific volume, the residual internal energy function is defined by Equation (36) [27]:

$$u_m - u_{m_{id}} = \int_{v_{m,l} \rightarrow \infty}^{v_m} \left[T \left(\frac{\partial P}{\partial T} \right)_{v_m} - P \right] dv_m \quad (36)$$

where

u_m —molar internal energy of real gas;

$u_{m_{id}}$ —molar internal energy of ideal gas.

By using Equation (28), the partial derivative in Equation (36) can be calculated from the following equation:

$$\left(\frac{\partial P}{\partial T} \right)_{v_m} = \left(\frac{\partial P}{\partial T} \right)_{\rho_m} = R \rho_m \left[Z + T \left(\frac{\partial Z}{\partial T} \right)_{\rho_m} \right] \quad (37)$$

By substituting Equation (37) in Equation (36) and by replacing the variable v_m with ρ_m , the equation will be obtained that will enable the calculation of the internal energy [49]:

$$u_m - u_{m_{id}} = -RT^2 \int_0^{\rho_m} \left(\frac{\partial Z}{\partial T} \right)_{\rho_m} \frac{d\rho_m}{\rho_m} \quad (38)$$

To calculate the molar internal energy of an ideal gas, the following equation was used:

$$u_{m_{id}} = h_{m_{id}} - pv_m = h_{m_{id}} - RT \quad (39)$$

In Equation (39), $h_{m_{id}}$ is the molar enthalpy of an ideal gas, calculated with the following equation:

$$h_{m_{id}} = \sum_{j=0}^n x_j h_{m,i}^j \quad (40)$$

where

$h_{m,i}^j$ —molar enthalpy for component j in the ideal gas mixture;

Internal energy per mass unit was calculated from Equation (41):

$$u = \frac{u_m}{M} \quad (41)$$

The procedure for calculating the selected properties of natural gas in a composite tank (type IV) begins with the indication of the initial conditions (pressure and temperature). The remaining initial thermodynamic properties, including the enthalpy of the reservoir tank $h_R = u_R + (pv)_R$, are calculated using the Peng–Robinson equation of state. Equation (2) or (3) is used to calculate the inlet mass flow. Equation (1) is used to calculate the natural gas mass in a composite tank (type IV), and then the specific volume of natural gas stored in the composite tank is calculated using the gas density. Equation (15) was solved to calculate the specific internal energy of natural gas in the composite tank in the new time period. When the specific internal energy and specific volume were deter-

mined, the remaining properties (e.g., compressibility factor, gas density, Joule–Thomson coefficient) were calculated using the P-R equation of state.

6. Results and Discussion

This study analyzes the scenario in which a composite tank was installed in a NGV and was considered as an adiabatic system. As a result of this assumption, the orifice diameter and the mass flow rate at the inlet to the composite tank have no effect on the final in-cylinder temperature and pressure. The orifice diameter and cylinder volume were assumed to be 1 mm and 50 L, respectively. It was also assumed that the discharge coefficient of the orifice C_d (at the inlet to the composite tank) is equal to one. The results are presented for a single reservoir tank as shown in Figure 3.

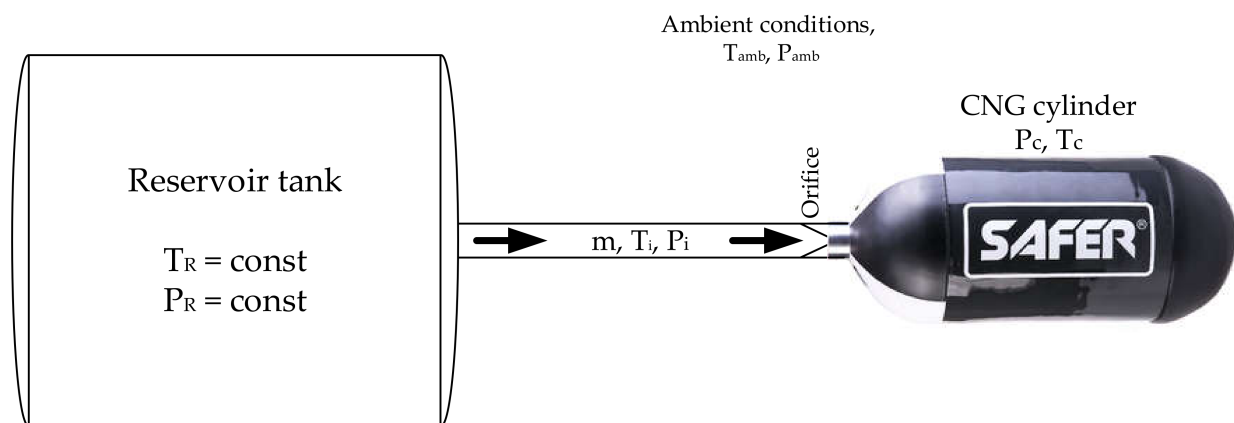


Figure 3. Thermodynamic scheme of the investigated system (buffer storage).

The Joule–Thomson coefficient μ_{J-T} plays an important role during the composite tank fast filling process. A gas with a positive μ_{J-T} coefficient cools down during the expansion. The change in temperature with respect to pressure is directly related to the value of the μ_{J-T} coefficient. It is advisable to determine this coefficient during the filling process of the composite tank [22,50].

Figure 4 shows the influence of natural gas composition on the μ_{J-T} coefficient in the cylinder during the filling process under the initial conditions of 300 K and 0.101325 MPa.

Data analysis presented in Figure 4 shows that in the initial stage of composite tank filling, there occurs an increase of the J-T coefficient. The J-T coefficient is positive throughout the filling process, so the gas temperature should decrease as the pressure decreases. Comparing the values of the J-T coefficient for different natural gas compositions, it can be noticed that μ_{J-T} is higher for mixtures with lower methane content in the composition (for gas samples 4, 3, 2). For nitrogen-rich gas (Gas sample 5), the J-T coefficient ratio is the lowest among the analyzed samples. The results obtained are consistent with those obtained by Farzaneh-Gord et al. 2014 [27]. The maximum value of J-T coefficient for pure methane is slightly higher—this can be a result of different initial pressure in the reservoir tank and the use of different EOS.

Figure 5 shows the influence of natural gas composition on the gas temperature inside the composite tank during the filling process (for the assumed initial conditions of $T = 300$ K and $p = 0.101325$ MPa). The analysis of the results shows that the temperature of the natural gas in the composite tank decreases at the beginning of the refueling process. The reason of the natural gas temperature drop at the early stage of composite tank filling is the Joule–Thomson effect which occurs during the isenthalpic expansion on the orifice (from the inlet pressure of 21 MPa which is set in the reservoir tank, to the initially low pressure in the composite tank 0.101325 MPa) [22,49]. During the fast filling process, the natural gas is injected to the composite tank, mixes with the gas initially contained in the tank, and compresses it. Since there is low pressure in the tank initially, this causes

that the temperature of the natural gas injected into the tank initially decreases due to isenthalpic expansion.

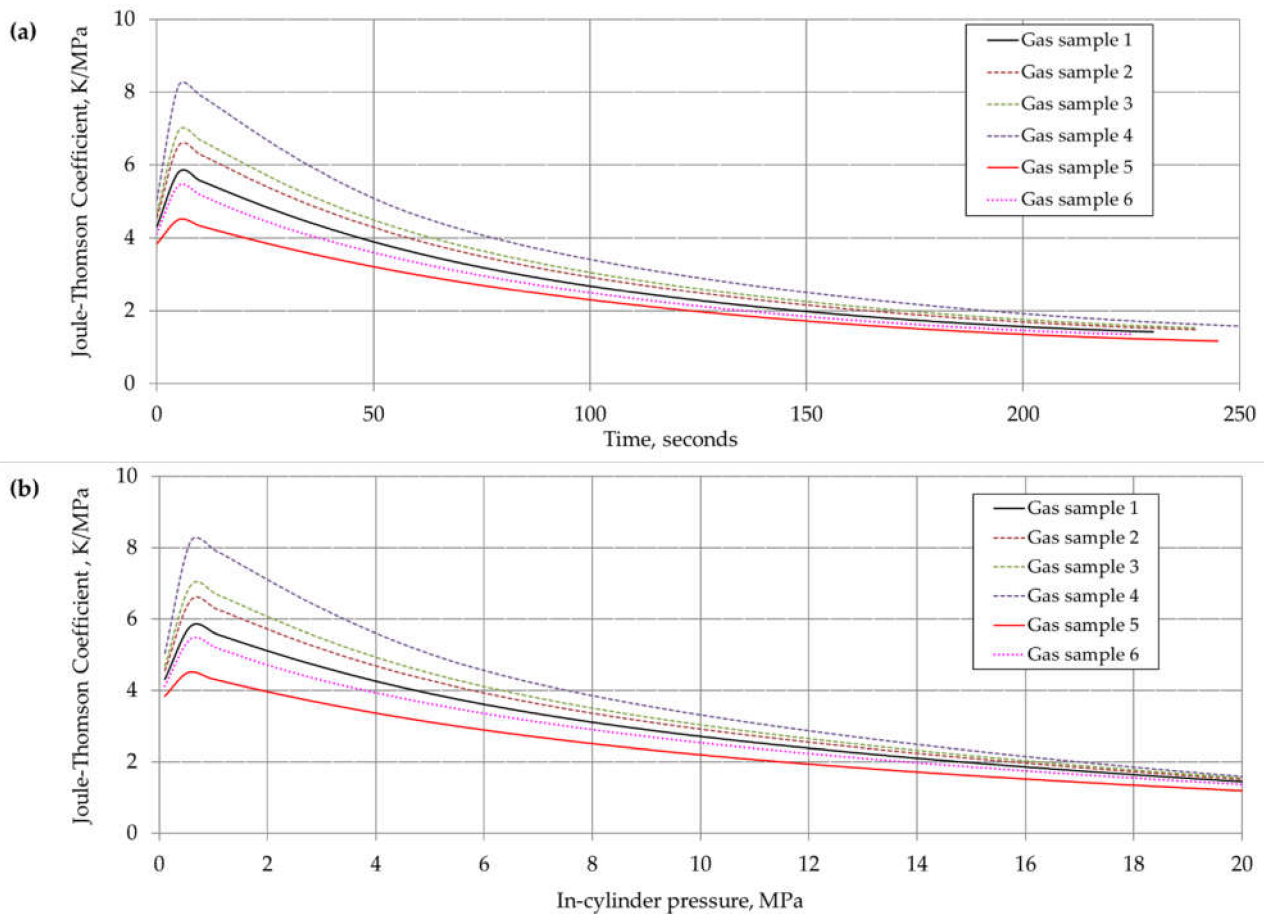


Figure 4. In-cylinder Joule–Thomson coefficient changes for the considered natural gas mixtures during the composite tank fast filling process: (a) vs. pressure change in the composite tank; (b) vs. filling time of the composite tank.

The lowest natural gas temperature in the composite tank occurs at the highest calculated J-T coefficient. When the compression process and the conversion of the supplied enthalpy to internal energy in the composite tank overcome the cooling effect of the Joule–Thomson effect (which decreases with the pressure increase in the cylinder), the temperature of the natural gas in the composite tank begins to increase. The gas temperature increases quickly as the initial quantity of gas in the composite tank is low and increases rapidly with the fueling process (Figure 5). The natural gas temperature increase in the composite tank during the fueling process slightly slows down due to the influence of lower ambient temperature and lower dynamics of the compression process in the final phase (decrease in mass fueling efficiency).

The analysis of the temperature profiles presented in Figure 5, shows that the lowest gas temperature during filling corresponds to the natural gas sample with the lowest methane content in the composition (Gas sample 4, for gas with the highest coefficient μ_{J-T}), but it should be noted that this does not apply to nitrogen-rich natural gas (Gas sample 5), where nitrogen significantly reduces the Joule–Thomson effect. At the end of the refueling process, a temperature difference of about 11 K occurs for the natural gas sample with the highest methane content (Gas sample 2) and the natural gas sample with the lowest methane content (Gas sample 4). It should also be noted that the maximum difference in the final gas temperature in the tank is higher, considering nitrogen-rich natural gas sample (Gas sample 5), which is 20 K. Obtained results are consistent with those presented in different articles [20,22,27]. The decrease of methane temperature at the beginning of the

filling process is slightly higher—this can be a result of different cylinder volume and the use of different EOS.

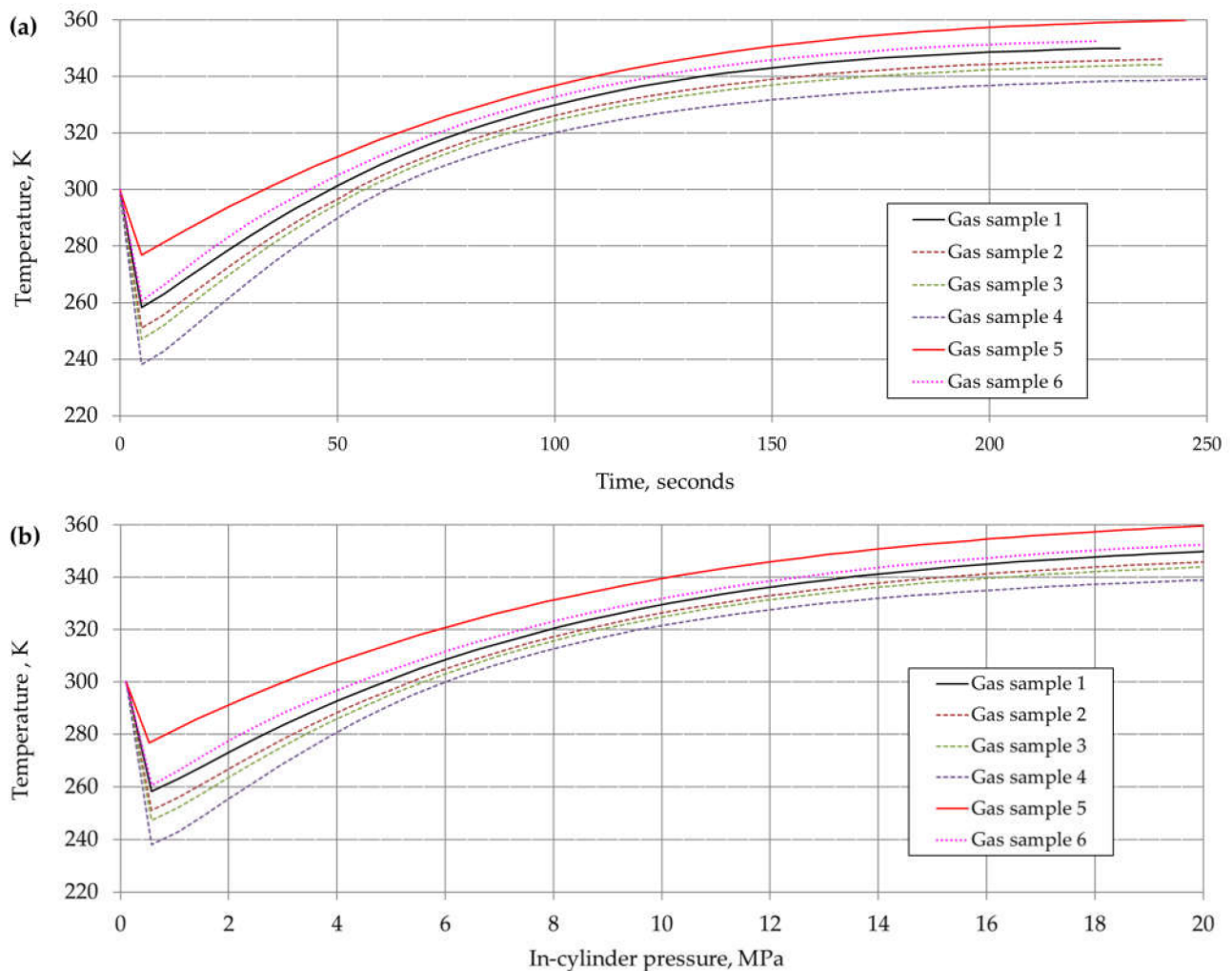


Figure 5. Temperature changes of the considered natural gas mixtures during the composite tank fast filling process: (a) vs. pressure change in the composite tank; (b) vs. filling time of the composite tank.

Figure 6 shows the mass flow rate profiles during the composite tank filling process for selected compositions of natural gas at constant initial conditions: ambient temperature $T = 300$ K and pressure $p = 0.101325$ MPa. Analysis of the results shows that at the early stage of filling, the mass flow rate is constant due to a choking effect formed on the tank orifice (inlet). The highest value of the mass flow rate occurs for the high-methane natural gas with the lowest content of methane in the composition (Gas sample 4). It is caused due to the higher density of natural gas with this composition.

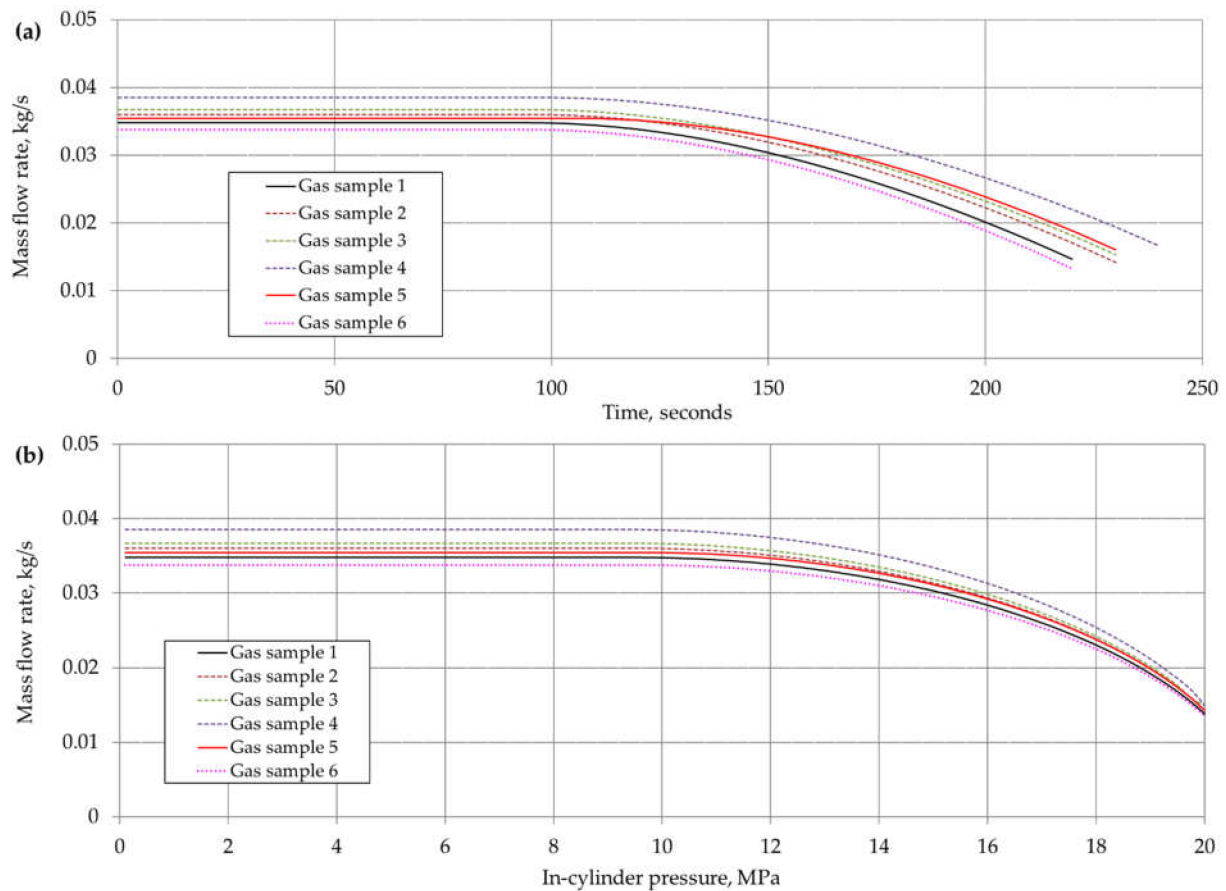


Figure 6. Mass flow rate change of the considered natural gas mixtures during the composite tank fast filling process: (a) vs. pressure change in the composite tank; (b) vs. filling time of the composite tank.

It should also be mentioned that nitrogen-rich gas (Gas sample 5) has the highest molar mass, but the mass flow rate is only slightly higher than in the case of pure methane, because nitrogen-rich gas has the highest compressibility factor among the selected samples. Figure 6 presents the effect of the natural gas composition on the mass flow profile during the composite tank filling process. Obtained results are consistent with those presented in other works [20,22,27]. The initial mass flow rate for methane is 0.035 kg/s. The time required to reach the final pressure (20 MPa) in the cylinder is about 220 s. Compared to other works, the filling time is shorter, due to the adoption of a smaller tank volume for the calculation.

Figure 7 shows the in-cylinder mass increase during the composite cylinder (type IV) fast filling process. The mass of gas in the composite tank is expected to be higher for the natural gas with higher density. The density is higher for a gas with a lower temperature and lower methane content. The gas temperature in the composite tank is also lower for low-methane gas (Gas samples 4, 3, 2), with no significant nitrogen content (see Figure 5). The final mass accumulated in the composite tank (after the filling process is complete) is slightly higher (0.5 kg) for nitrogen-rich natural gas with the lowest content of methane (Gas sample 5) compared to pure methane. In the case of high-methane gas with the lowest methane content (Gas sample 4), the weight of compressed natural gas is about 1.2 kg more than in the case of pure methane. This relationship shows the significant influence of natural gas composition on the fast filling process of a composite tank (type IV).

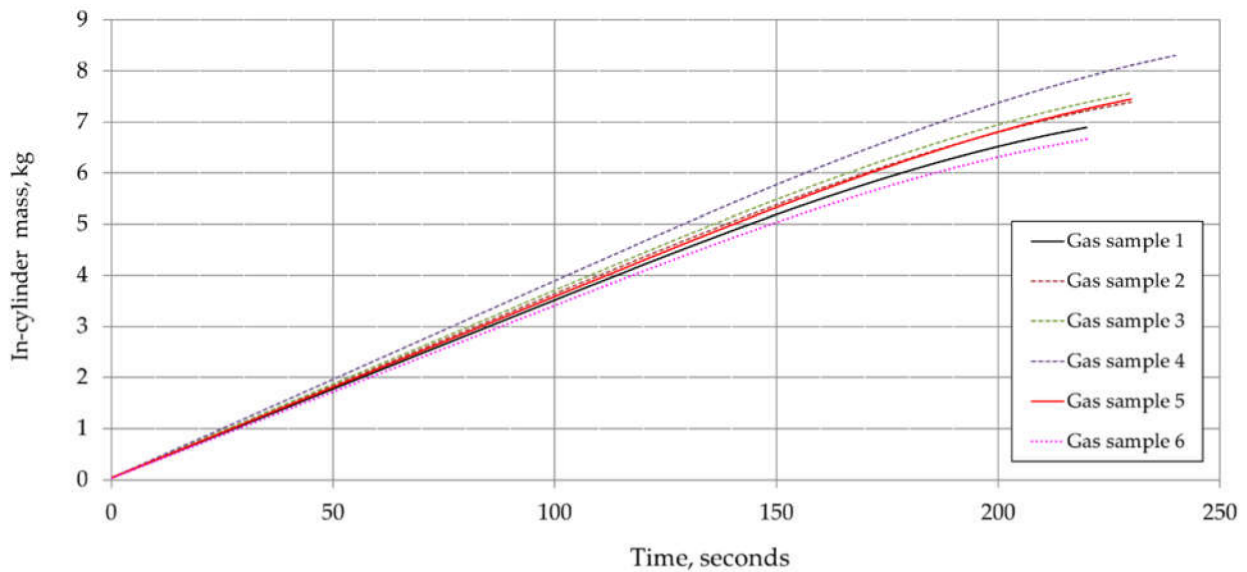


Figure 7. In-cylinder mass increase for the considered natural gas mixtures during the fast filling process of the composite tank (type IV).

Figure 7 shows the effect of natural gas composition on the composite tank filling time. The analysis shows that there is difference between the time profiles for the different natural gas compositions. The slight influence of the gas composition on the filling time results in two opposing effects. The mass flow rate at the inlet of the composite tank for gas with a lower methane content is higher (Gas sample 4), so the time should be shorter (not for nitrogen-rich gas). On the other hand, the mass accumulated in the cylinder is greater for such gas, so it takes more time to fill the composite tank. Obtained results are consistent with those presented in other works [20,22,27]. The final in-cylinder mass of methane is about 7 kg, reached after about 220 s. Compared this result with other works, the filling time is shorter, due to the conjunction with a smaller tank volume for the calculation (50 l tank in this work vs. 67 l) and thus a lower accumulated mass of methane (7 kg in this work vs. 8 kg).

Figure 8 shows the profiles of natural gas density changes in the composite tank during the fueling process. The results for the obtained profiles of density changes are consistent with the profiles of gas mass increase in the tank (Figure 7).

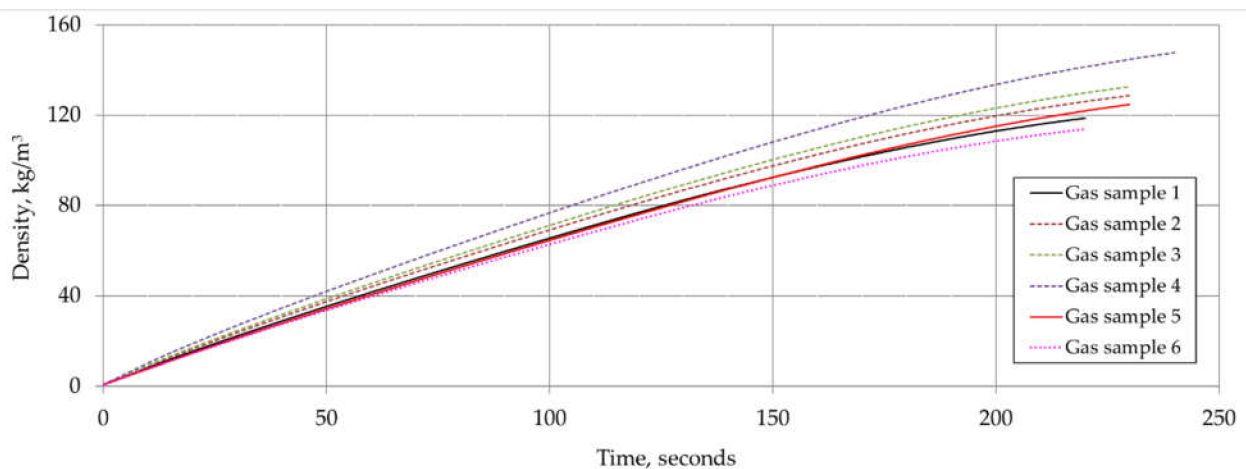


Figure 8. Density profiles for the considered natural gas mixtures during the fast filling process of the composite tank (type IV).

Figure 9 shows the influence of the ambient temperature on the final natural gas temperature for the various gas compositions at the end of fast filling process. The analysis of the results shows that the final gas temperature in the composite tank is the highest for nitrogen-rich gas (Gas sample 5). Natural gas mixtures with a higher percentage of methane also exhibit high final temperatures (including methane and methane with 3% hydrogen blend).

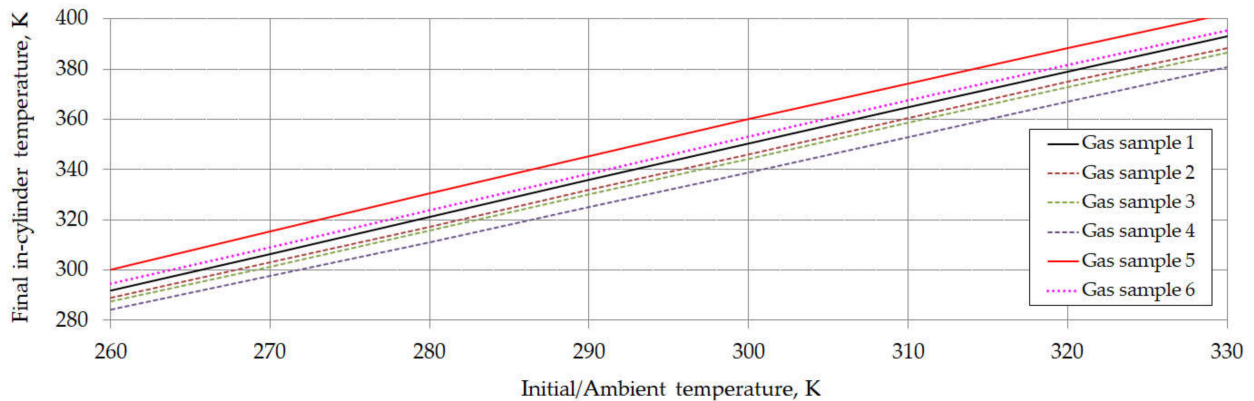


Figure 9. Influence of initial temperature (ambient) on the final in-cylinder temperature for the considered natural gas mixtures.

Mixtures of natural gas samples 4, 3, and 1 showed the lowest values of the final gas temperature after the filling process. It is essential that increasing the initial ambient temperature causes a linear increase of the final gas temperature in the composite tank. Moreover, other studies [25] showed that the initial gas temperatures in the tank (type III and type IV) and in the reservoir tank (ambient temperature) have an important impact on the natural gas properties after composite tank fast filling completion. Obtained results are consistent with those presented in other works [20,22]. The final in-cylinder temperature for methane is about 350 K, with the initial gas temperature 300 K. Comparing this result with the other, it shows that the final in-cylinder temperature is similar.

Figure 10 shows the effect of an ambient temperature (corresponding to the gas temperature) on the amount of gas mass filled into the composite tank—for different natural gas compositions. As mentioned earlier, the amount of gas filled into the composite tank has a direct impact on the range of the NGV and is one of the major problems associated with the NGV industry.

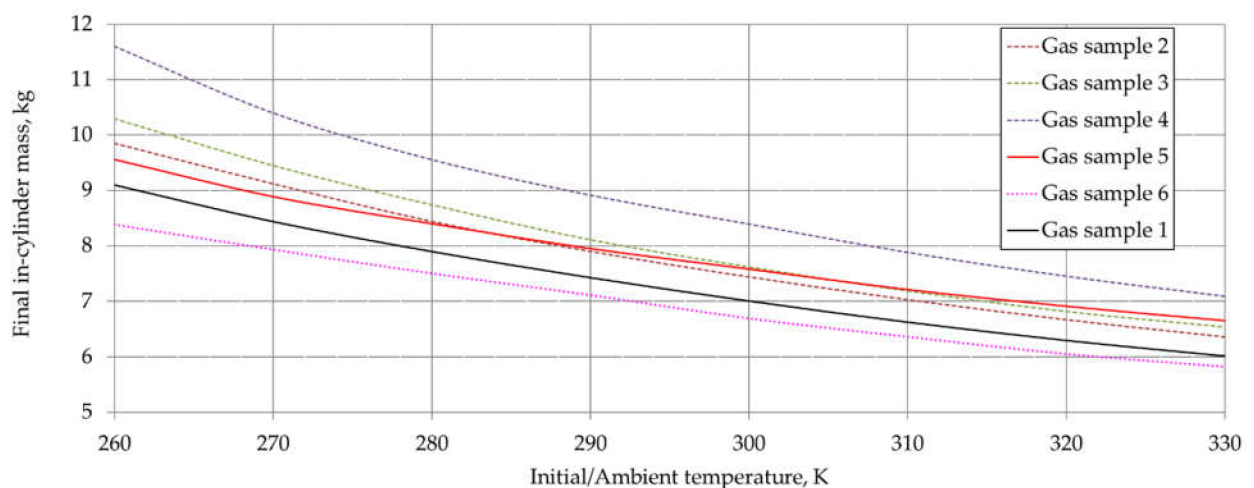


Figure 10. Influence of the initial (ambient) temperature on the mass of fueled natural gas mixtures and samples.

The analysis showed that the mass of the fueled gas decreases with the increase of the ambient temperature in which the process of the composite tank filling has been carried out. It can be observed that the difference of the fueled mass for the considered different natural gas compositions decreases with the ambient temperature increase. As the ambient temperature decreases, the amount of gas refilled into the composite tank increases, so it can be concluded that the tanks should be filled at lower ambient temperatures (rather at night than during the day). The weight of the fueled gas is the highest for the gas mixtures with the highest density (Gas samples 4, 3, 2). For nitrogen-rich gas, due to the higher compressibility factor, the mass of the refueled natural gas (Gas sample 5) decreases slower with the increase of the ambient temperature. Obtained results are consistent with those presented in other works [22,27]. The final in-cylinder mass of methane (Gas sample 1) is about 7 kg for the initial gas temperature 300 K. Comparing this result to the other, it shows that the final in-cylinder mass is higher, due to the conjunction with a smaller tank volume for the calculation (50 l tank in this work vs. 67 l) and thus a lower accumulated mass of methane (7 kg in this work vs. 8 kg).

7. Conclusions

In this study, the first law of thermodynamics and continuity equations were applied to develop a theoretical model to investigate the effects of natural gas composition on the filling process and the final in-cylinder conditions of NGV on-board composite cylinder (type IV). Properties of various gas samples were calculated with PR EOS. Samples were selected based on the composition which occurs in the Polish distribution and transmission system. The results of this study show that: (i) J-T coefficient is higher for mixtures with a lower methane content in the composition; (ii) at the end of the refueling process, the maximum difference in the final gas temperature in the tank is higher, considering nitrogen-rich gas sample, which is 20 K; (iii) the highest value of the mass flow rate occurs for the high-methane natural gas with the lowest content of methane in the composition (Gas sample 4); (iv) for high-methane gas with the lowest methane content (Gas sample 4), the weight of compressed natural gas is about 1.2 kg more than in the case of pure methane; (v) increase in the initial ambient temperature causes a linear increase of the final gas temperature in the composite tank, which in this study is highest for nitrogen-rich natural gas (Gas sample 5); (vi) analysis of influence of an ambient temperature on the amount of the refueled natural gas mass showed that the weight of the fueled gas is the highest for the natural gas mixtures with the highest density (Gas samples 4, 3, 2). For nitrogen-rich natural gas, due to the higher compressibility factor, the mass of the refueled gas (Gas sample 5) decreases slower with the increase of the ambient temperature.

Main practical aspects of this research are related to the influence of natural gas composition on the fast-refueling process. Composition of natural gas has an influence on the time of fast-filling NGV cylinder and compressor performance due to the filling process. This process should be as short as possible and during this time the tank should be filled with as much gas as possible. The temperature of CNG during the filling process is essential to the final process conditions and process safety standards. Furthermore, the charged mass is different for each natural gas composition and it has a direct influence on the driving range.

These results emphasize the importance of natural gas composition as an important parameter for investigating the filling process of the NGV on-board composite tank (type IV) as a practical issue.

In the next research step, the authors plan to perform experimental tests on the developed ultralight composite tanks (type IV) that will allow calibration of the model (i.e., measurements of in-cylinder pressure and temperature).

Author Contributions: Conceptualization, S.K., T.W. and P.S.; methodology, S.K. and T.W.; validation, S.K. and T.W.; investigation, S.K.; resources, S.K.; data curation, T.W. and S.K.; writing—original draft preparation, S.K. and T.W.; writing—review and editing, A.S. (Adam Saferna), P.S., M.L. and A.S. (Adam Szurlej); visualization, T.W. and S.K.; supervision, S.K.; funding acquisition, A.S. (Adam Saferna) and P.S. All authors have read and agreed to the published version of the manuscript.

Funding: This research was supported by RPO WM, RPMP.01.02.01-IP.01-12-072/18.

Acknowledgments: Special thanks to Piotr Ryba.

Conflicts of Interest: The authors declare no conflict of interest.

Nomenclature

Symbols

A	Area (m ²)
A, B	dimensionless Peng–Robinson EOS coefficients
a_i, b_i	Peng–Robinson EOS constants
C_d	Orifice discharge coefficient
C_p	Isobaric heat capacity (kJ/kg·K)
C_v	Isochoric heat capacity (kJ/kg·K)
g	Gravitational acceleration (m/s ²)
h	Specific enthalpy (kJ/kg)
h_m	Molar enthalpy (kJ/kmol)
\dot{m}	Mass flow rate (kg/s)
M	Molecular weight (kg/kmol)
p	Pressure (bar or Pa)
\dot{Q}	Heat transfer rate (kW)
R	universal gas constant (kJ/(kmol·K))
t	Time (s)
T	Temperature (K or °C)
u	Internal energy (kJ/kg)
u_m	Molar internal energy
U_{HC}	Heat transfer coefficient (W/(m ² K))
v	Specific volume (m ³ /kg)
v_m	Molar specific volume (m ³ /mol)
V	Velocity (m/s)
W	Actual work (kJ/kg)
\dot{W}	Actual work rate (kW or MW)
z	Height (m)
Z	Compressibility factor

Greek letters

α	Soave alpha function
δ_{ij}	Binary coefficient
ρ	Density (kg/m ³)
ρ_m	Molar density (mol/m ³)
ρ_r	Reduce density
γ	Isentropic exponent
μ_{J-T}	Joule–Thomson coefficient (K/MPa)
ω	Acentric factor

Subscripts

C	NGV onboard cylinder
<i>cr</i>	Critical
<i>cv</i>	Control volume
R	Reservoir tank
<i>id</i>	Ideal gas
<i>I</i>	Initial or inlet condition
<i>r</i>	Recent
<i>res</i>	Residual
S	Start of filling process
<i>amb</i>	Ambient
<i>av</i>	Average

References

- Kuczyński, S.; Liszka, K.; Łaciak, M.; Kyć, K.; Oliinyk, A.; Szurlej, A. The impact of the use of alternative fuels in transport, with a particular emphasis on CNG, to reduce the emissions of air pollutants. *Polityka Energetyczna—Energy Policy J.* **2016**, *19*, 91–104.
- Khan, M.I.; Yasmin, T.; Shakoor, A. Technical overview of compressed natural gas (CNG) as a transportation fuel. *Renew. Sustain. Energy Rev.* **2015**, *51*, 785–797. [[CrossRef](#)]
- Burchart-Korol, D.; Gazda-Grzywacz, M.; Zarebska, K. Research and Prospects for the Development of Alternative Fuels in the Transport Sector in Poland: A Review. *Energies* **2020**, *13*, 2988. [[CrossRef](#)]
- NGV Global. Statistics on Natural Gas Vehicles. Available online: www.ngvglobal.org/ngv-statistics/ (accessed on 26 July 2021).
- IGU. Global Gas Report 2018. In Proceedings of the 27th World Gas Conference, Washington, DC, USA, 23–29 June 2018.
- IEA. *Natural Gas Information 2020*; International Energy Agency: Paris, France, 2020.
- PSPA. Rynek Paliw Alternatywnych CNG i LNG. In *Polskie Stowarzyszenie Paliw Alternatywnych*; PSPA: Warszawa, Poland, 2017.
- Nagy, S.; Siemek, J. Shale gas in Europe: The state of the technology-challenges and opportunities. *Arch. Min. Sci.* **2011**, *56*, 727–760.
- Siemek, J.; Kaliski, M.; Rychlicki, S.; Sikora, S.; Janusz, P.; Szurlej, A. Importance of LNG technology in the development of world's natural gas deposits. *Gospod. Surowcami Miner.* **2011**, *27*, 109–130.
- Dorosz, P. Sprężony i skroplony gaz ziemny jako alternatywa dla paliw ropopochodnych wykorzystywanych w transporcie. *Polityka Energetyczna—Energy Policy J.* **2018**, *21*, 85–98.
- European Parliament and the Council of the European Union, Deployment of Alternative Fuels Infrastructure, Directive 2014/94/EU. 2014. Official Journal of the European Union. Available online: <https://eur-lex.europa.eu/legal-content/EN/TXT/?uri=celex%3A32014L0094> (accessed on 30 August 2021).
- European Parliament and the Council of the European Union, Union Guidelines for the Development of the Trans-European Transport Network and Repealing Decision No 661/2010/EU, Regulation (EU) No 1315/2013. 2013. Official Journal of the European Union. Available online: https://eur-lex.europa.eu/legal-content/EN/TXT/?uri=uriserv:OJ.L_.2013.348.01.0001.01.ENG (accessed on 30 August 2021).
- Communication from the Commission. *The European Green Deal*; European Commission: Brussels, Belgium, 2019; Available online: <https://eur-lex.europa.eu/legal-content/EN/TXT/?uri=COM%3A2019%3A640%3AFIN> (accessed on 30 August 2021).
- Speirs, J.; Balcombe, P.; Blomerus, P.; Stettler, M.; Brandon, N.; Hawkes, A. Can natural gas reduce emissions from transport. In *Heavy Goods Vehicles and Shipping*; Sustainable Gas Institute, Imperial College London: London, UK, 2019.
- Ogden, J.; Jaffe, A.M.; Scheitrum, D.; McDonald, Z.; Miller, M. Natural gas as a bridge to hydrogen transportation fuel: Insights from the literature. *Energy Policy* **2018**, *115*, 317–329. [[CrossRef](#)]
- International Standard. ISO 11439-2013. *Gas Cylinders—High Pressure Cylinders for the On-Board Storage of Natural Gas as a Fuel for Automotive Vehicles*; ISO: Geneva, Switzerland, 2013.
- European Standard. EN 12245-2011, *Transportable Gas Cylinders. Fully Wrapped Composite Cylinders*; European Standards: Brussels, Belgium, 2011.
- Regulation No 110 of the Economic Commission for Europe of the United Nations (UN/ECE)—Uniform Provisions Concerning the Approval of I. Specific Components of Motor Vehicles Using Compressed Natural Gas (CNG) in Their Propulsion System; II. Vehicles with Regard to the Installation of Specific Components of an Approved Type for the Use of Compressed Natural Gas (CNG) in Their Propulsion System. 2010. Official Journal of the European Union. Available online: [https://eur-lex.europa.eu/legal-content/EN/TXT/?uri=CELEX:42011X0507\(01\)](https://eur-lex.europa.eu/legal-content/EN/TXT/?uri=CELEX:42011X0507(01)) (accessed on 30 August 2021).
- Kountz, K.J. Modeling the fast fill process in natural gas vehicle storage cylinders. In Proceedings of the 207th ACS National Meeting-Division of Fuel Chemistry, San Diego, CA, USA, 13–17 March 1994; Institute of Gas Technology: Chicago, IL, USA, 1994.
- Farzaneh-Gord, M.; Deymi-Dashtebayaz, M.; Rahbari, H.R. Studying effects of storage types on performance of CNG filling stations. *J. Nat. Gas Sci. Eng.* **2011**, *3*, 334–340. [[CrossRef](#)]
- Farzaneh-Gord, M. Real and ideal gas thermodynamic analysis of single reservoir filling process of natural gas vehicle cylinders. *J. Theor. Appl. Mech.* **2011**, *41*, 21–36.

22. Deymi-Dashtebayaz, M.; Farzaneh-Gord, M.; Rahbari, H.R. Studying transmission of fuel storage bank to NGV cylinder in CNG fast filling station. *J. Braz. Soc. Mech. Sci. Eng.* **2012**, *34*, 429–435. [[CrossRef](#)]
23. Farzaneh-Gord, M.; Deymi-Dashtebayaz, M. Optimizing natural gas fueling station reservoirs pressure based on ideal gas model. *Pol. J. Chem. Technol.* **2013**, *15*, 88–96. [[CrossRef](#)]
24. Farzaneh-Gord, M.; Deymi-Dashtebayaz, M.; Rahbari, H.R. Effects of gas types and models on optimized gas fuelling station reservoir's pressure. *Braz. J. Chem. Eng.* **2013**, *30*, 399–411. [[CrossRef](#)]
25. Nahavandi, N.N.; Farzaneh-Gord, M. Numerical simulation of filling process of natural gas onboard vehicle cylinder. *J. Braz. Soc. Mech. Sci. Eng.* **2013**, *35*, 247–256. [[CrossRef](#)]
26. Deymi-Dashtebayaz, M.; Farzaneh-Gord, M.; Nooralipoor, N.; Rastgar, S. The full simulation of rapid refueling of a natural gas vehicle on-board cylinder. *J. Nat. Gas Sci. Eng.* **2014**, *21*, 1099–1106. [[CrossRef](#)]
27. Farzaneh-Gord, M.; Rahbari, H.R.; Deymi-Dashtebayaz, M. Effects of natural gas compositions on CNG fast filling process for buffer storage system. *Oil Gas Sci. Technol.—Rev. D'ifp Energ. Nouv.* **2014**, *69*, 319–330. [[CrossRef](#)]
28. Khamforoush, M.; Moosavi, R.; Hatami, T. Compressed natural gas behavior in a natural gas vehicle fuel tank during fast filling process: Mathematical modeling, thermodynamic analysis, and optimization. *J. Nat. Gas Sci. Eng.* **2014**, *20*, 121–131. [[CrossRef](#)]
29. Ramoutar, S.; Riverol, C.A. Thermodynamic analysis of refueling a Natural Gas Vehicle cylinder from a cascade reservoir using chilled natural gas. *J. Nat. Gas Sci. Eng.* **2017**, *38*, 298–322. [[CrossRef](#)]
30. Zhang, G.; Brinkerhoff, J.; Li, R.; Forsberg, C.; Sloan, T. Analytical and numerical study on the fast refill of compressed natural gas with active heat removal. *J. Nat. Gas Sci. Eng.* **2017**, *45*, 552–564. [[CrossRef](#)]
31. Taccani, R.; Maggiore, G.; Micheli, D. Development of a Process Simulation Model for the Analysis of the Loading and Unloading System of a CNG Carrier Equipped with Novel Lightweight Pressure Cylinders. *Appl. Sci.* **2020**, *10*, 7555. [[CrossRef](#)]
32. Liu, J.; Zheng, S.; Zhang, Z.; Zheng, J.; Zhao, Y. Numerical study on the fast filling of on-bus gaseous hydrogen storage cylinder. *Int. J. Hydrogen Energy* **2020**, *45*, 9241–9251. [[CrossRef](#)]
33. Dicken, C.J.B.; Merida, W. Modeling the transient temperature distribution within a hydrogen cylinder during refueling. *Numer. Heat Transf. Part A Appl.* **2007**, *53*, 685–708. [[CrossRef](#)]
34. Bourgeois, T.; Ammouri, F.; Weber, M.; Knapik, C. Evaluating the temperature inside a tank during a filling with highly-pressurized gas. *Int. J. Hydrogen Energy* **2015**, *40*, 11748–11755. [[CrossRef](#)]
35. Deymi-Dashtebayaz, M.; Farzaneh-Gord, M.; Nooralipoor, N.; Niazmand, H. The complete modelling of the filling process of hydrogen onboard vehicle cylinders. *Braz. J. Chem. Eng.* **2016**, *33*, 391–399. [[CrossRef](#)]
36. Wang, L.; Zheng, C.; Wei, S.; Wang, B.; Wei, Z. Thermo-mechanical investigation of composite high-pressure hydrogen storage cylinder during fast filling. *Int. J. Hydrogen Energy* **2015**, *40*, 6853–6859. [[CrossRef](#)]
37. Khab, H.; Chaker, A.; Ziani, L. Effects of pressure and hydrogen addition to methane on the temperatures within a pressurized cylinder during the vehicle refueling of HCNG. *Int. J. Hydrogen Energy* **2019**, *44*, 22437–22444. [[CrossRef](#)]
38. Bourgeois, T.; Ammouri, F.; Baraldi, D.; Moretto, P. The temperature evolution in compressed gas filling processes: A review. *Int. J. Hydrogen Energy* **2018**, *43*, 2268–2292. [[CrossRef](#)]
39. Li, H.; Lyu, Z.; Liu, Y.; Han, M.; Li, H. The effects of infill on hydrogen tank temperature distribution during fast fill. *Int. J. Hydrogen Energy* **2021**, *46*, 10396–10410. [[CrossRef](#)]
40. Bai, Y.; Zhang, C.; Duan, H.; Jiang, S.; Zhou, Z.; Grouset, D.; Zhang, M.; Ye, X. Modeling and optimal control of fast filling process of hydrogen to fuel cell vehicle. *J. Energy Storage* **2021**, *35*, 102306. [[CrossRef](#)]
41. Sadi, M.; Deymi-Dashtebayaz, M. Hydrogen refueling process from the buffer and the cascade storage banks to HV cylinder. *Int. J. Hydrogen Energy* **2019**, *44*, 18496–18504. [[CrossRef](#)]
42. Melideo, D.; Baraldi, D.; Acosta-Iborra, B.; Cebolla, R.O.; Moretto, P. CFD simulations of filling and emptying of hydrogen tanks. *Int. J. Hydrogen Energy* **2017**, *42*, 7304–7313. [[CrossRef](#)]
43. Kuczyński, S.; Liszka, K.; Łaciak, M.; Oliynyk, A.; Szurlej, A. Experimental Investigations and Operational Performance Analysis on Compressed Natural Gas Home Refueling System (CNG-HRS). *Energies* **2019**, *12*, 4511. [[CrossRef](#)]
44. Safronov, A.; Guzeyeva, J.; Begens, J.; Mezulis, A. The Innovative Technology of Hydraulic Compression and Boosting for Filling the Vehicles and Storage Systems with Natural Gas and Biomethane. *Environ. Clim. Technol.* **2020**, *24*, 80–93. [[CrossRef](#)]
45. Nagy, S.; Barczyński, A.; Blicharski, J.; Duliński, W.; Łaciak, M.; Marszałek, J.; Ropa, C.E.; Rybicki, C.; Smulski, R.; Ślizowski, J.; et al. *Vademecum gazownika tom I. Podstawy Gazownictwa Ziemi: Pozyskiwanie, Przygotowanie do Transportu, Magazynowanie*; Scientific and Technical Association of Engineers and Technicians of the Oil and Gas Industry: Kraków, Poland, 2014.
46. Nederstigt, P. Real Gas Thermodynamics: And the Isentropic Behavior of Substances. Master's Thesis, Master of Science in Mechanical Engineering, Delft University of Technology, Delft, The Netherlands, 2017.
47. Peng, D.Y.; Robinson, D.B. A New Two-Constant Equation of State. *Ind. Eng. Chem. Fundam.* **1976**, *15*, 59–64. [[CrossRef](#)]
48. Chase, M. *NIST-JANAF Thermochemical Tables*, 4th ed.; American Chemical Society and the American Institute of Physics for the National Institute of Standards and Technology: New York, NY, USA, 1998; pp. 1–1951.
49. Moran, M.J.; Shapiro, H.N. *Fundamentals of Engineering Thermodynamics*, 6th ed.; John Wiley & Sons Inc.: Hoboken, NJ, USA, 2007.
50. Tsuchiya, M.; Ogasa, H.; Matsuura, H.; Shimanuki, H.; Fujii, I. *Thermodynamic Behavior of Supply Gas and Influence on Vehicle Fuel Fill Line during CNG Fast Fill*; SAE Technical Paper 961173; SAE International: Warrendale, PA, USA, 1996.